International Journal of Engineering and Information Systems (IJEAIS)
ISSN: 2000-000X
Vol. 1 Issue 7, September – 2017, Pages: 11-27

Structural, Magnetic and Transport Properties of Fe-deficient of Ni-Cu-Zn Ferrites

S. K. Bahadur[1] .M. A. Hossain[2]*, S. S. Sikder[3], M. S. Akhter[4]
Department of Physics Khulna University of Engineering & Technology KUET, Khulna Bangladesh[1,2,3]
Department of Material Science Atomic Energy Center, Dhaka, Bangladesh[4]
Corresponding author's email: liton@phy.kuet.ac.bd.com

Abstract: *The present work is focused on the influence on electromagnetic and transport properties of Fe-deficient Ni-Cu–Zn ferrites. These are ferrite samples of composition* $(Ni_{0.28}Cu_{0.10}Zn_{0.62}O)(Fe_2O)_{1-x}$ *where x = 0.00, 0.02, 0.04, 0.06 and 0.08 were prepared using the solid state reaction technique. The phase identification was carried out by X-ray diffraction. The X–ray diffraction analysis revealed that the samples crystallize in single phase cubic spinel structure. A slight increase of Curie temperature* (T_c)*, saturation magnetization* (M_s) *and initial permeability* (μ') *with increase of Fe-deficient. The permeability spectrum with frequency follows the Snoek's limit. Sample with x = 0.00 sintered at* 1100^0C *possess the maximum value of relative quality factor (RQF). From the B–H loops, the romance* (B_r) *and coercive force* (H_c) *were determined. Saturation induction* (B_s) *and* $\frac{B_r}{B_s}$ *are measured from low field B–H loops is found to increase with increasing Fe-deficient up to x = 0.04 thereafter decrease. DC resistivity increase with increasing Fe-deficient up to x = 0.06 and thereafter decrease. The dielectric constant is found to decrease continuously with increasing frequency and remains almost constant at higher frequency range. From hysteresis parameter it was revealed that optimum soft magnetic properties corresponds to the composition with x = 0.06 sintered at* 1100^0C *having highest permeability, maximum induction, minimum coercivity and hysteresis losses.*

Keywords: Solid State Reaction Technique, B–H loops, Permeability, Saturation Magnetization.

1. INTRODUCTION

The term ferrite denotes a group of iron oxides, which have the general formula $MO.Fe_2O_3$, where M is a divalent metal ion such as Mn^{2+}, Fe^{2+}, Co^{2+}, Ni^{2+}, Cu^{2+}, Zn^{2+}, Mg^{2+} or Cd^{2+}. Ferrite exhibits a spontaneous magnetization at room temperature, like ferromagnetic materials. They consists of spontaneously magnetized domains, show the phenomenon of magnetic saturation and hysteresis loop, and have a critical temperature T_C, called Curie temperature. These are of very high resistivity such as $10^2 - 10^{10}$ $\Omega - Cm$ which is very high than that of iron.

This outstanding property of ferrites makes them highly demandable for high frequency applications. This fact way first mentioned by S. Hilpert [1]. Now-a-days ferrites are employed truly in a wide range of applications, and have contributed to the advances in electronics like as transformer cores, inductors, high quality filters, radio frequency circuits, rod antennas, read/write heads for high speed digital tape and operating devices [2-4].

The ferrites were developed into commercially important materials chiefly during the year 1933-1945 by Sonek [5] and his associates at the Philips Research Laboratories in Holland. In a classical paper published in 1948 Neel [6] provided the theoretical key to an understanding of the ferrites.

Nakamura [7] reported on frequency dispersion of permeability in ferrite composite materials. The permeability increases with increasing density of composite materials. As the ferrite content decreases, both the shoulder frequency of real part of permeability dispersion; both the real and imaginary parts of the low frequency permeability is significantly reduced, and the peak frequency of imaginary part of permeability shifts toward higher frequency. Nakamura et al [8] reported on low temperature sintering Ni-Cu-Zn ferrite and its permeability spectra. The post sintering density and the complex permeability Ni-Cu-Zn ferrite ceramic can be controlled by altering the particle size of the sintering oxide materials and calcinations temperature.

Ni-Cu-Zn ferrites are widely used multilayer chip devices. These devices were studied by K. O. low and F. R. Sale [9], such as multilayer chip inductors, are produced by Co-firing ferrite layers with an internal silver conductor. The low sintering temperature is attributed to its Cu-content because the Cu-containing ferrites were claimed to suffer thermal dissociation at temperature around 990^0C. Kin O. Low et al. [10] has design of Ni-Cu-Zn ferrites to suit a particular application where consideration was given on thermal dissociation temperature so that electromagnetic properties are not affected. Rahman et al. [11] studied on Ni-Cu-Zn based ferrite. Average crystalline size increase linearly with calcinations temperature, the lattice parameter and the ionic radius of octahedral sites increases with copper concentrations. The saturation magnetization decreases with increasing non magnetic Cu-content.

The extensive literature survey reveals that the synthesis of crystalline Ni-Cu-Zn ferrite powder through solid state method has been attempted by a number of researchers. The electromagnetic properties have been reported with various Fe

concentrations in Ni-Cu-Zn ferrites [12-13]. Optimization of Fe concentration with respect to Ni, Cu and Zn is essential to achieve desirable electromagnetic properties in the ferrites.

2. Materials and Methods

Ferrites with optimized properties are always demanded delicate handling and caution approach in materials synthesis and appropriate knowledge of thermodynamics control of the chemical composition and homogeneity. There are many processing methods such as solid state reaction method [14], high energy ball milling [15], sol gel method [16], chemical co-precipitation method [17], microwave sintering method [18], auto combustion method [19] etc for the preparation of polycrystalline ferrite materials

The weight percentage of the oxide to be mixed for various samples was calculated by using formula:

$$\text{Weight \% of oxide} = \frac{M.wt \cdot of\ oxide \times required\ \ weight\ of\ the\ sample}{Sum\ of\ Mol.wt.of\ each\ oxide\ in\ a\ sample}$$

In Solid State Reaction Method, different metal oxide and rare earth metal oxides are mixed and calcined to get ferrite powders. However mechanical mixing of different oxides is hardly intimate and homogeneous and hence its results in composition fluctuation at every stage of processing that also persist after sintering Chen [20]. Solid state process requires calcinations temperature more than 600^0C for phase formation and sintering temperature more than 1000^0C to achieve better densification. This high sintering temperature evaporation of Zn leads to the formation of chemically inhomogeneous material Goldman [21]. The ferrite is not completely defined by its chemistry and crystal structure but also requires knowledge and control of parameters of its microstructure such as grain size, porosity, intra and intergranular distribution.

The following block diagram in represents the method employed for the rare - earth ferrites:

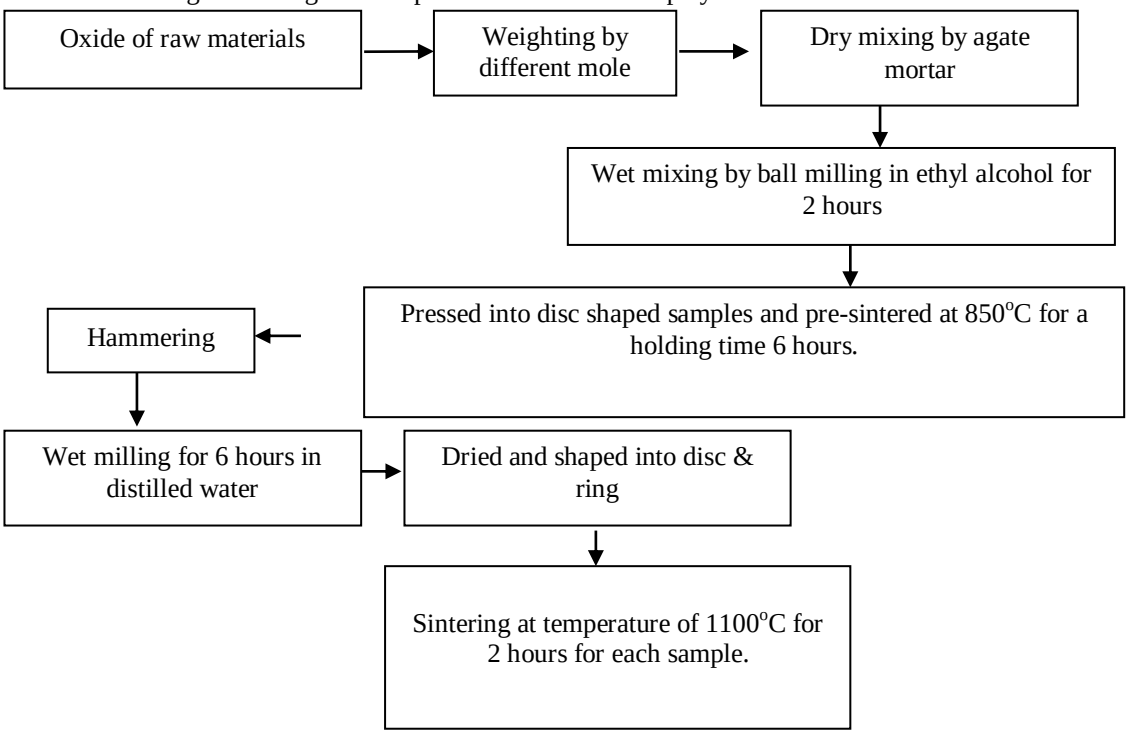

3. Results and Discussion

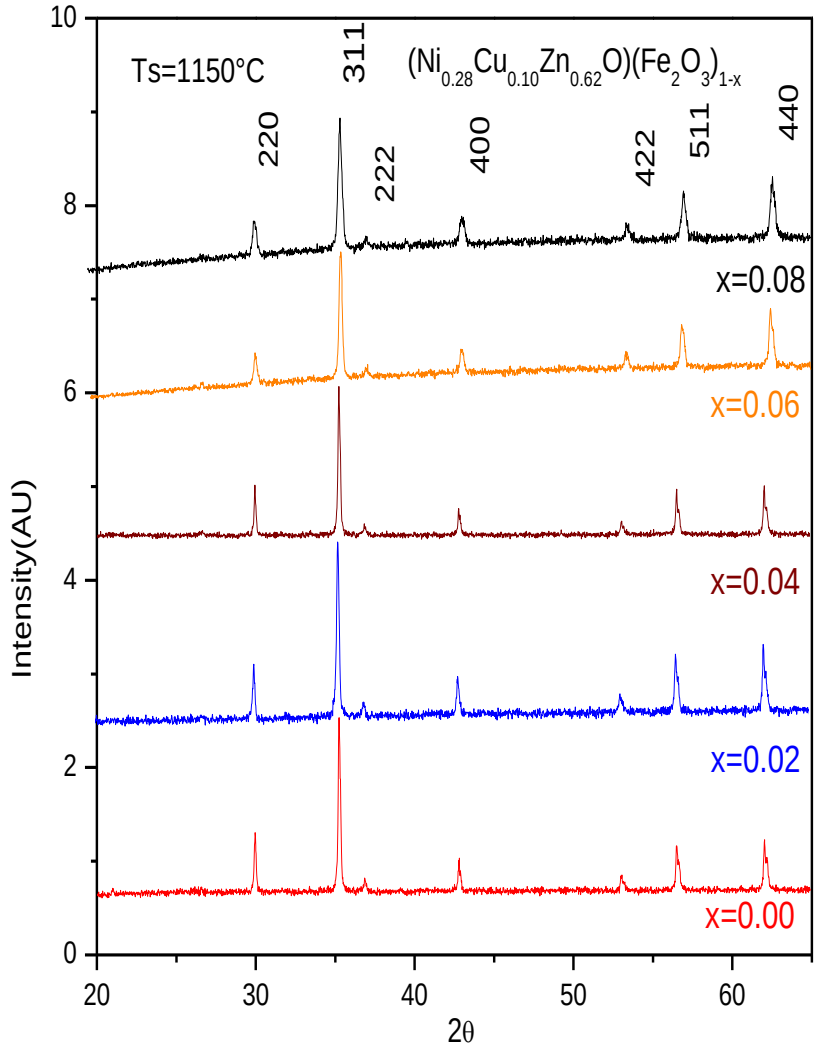

Figure-1 X-ray diffraction patterns of $(Ni_{0.28}Cu_{0.10}Zn_{0.62}O)(Fe_2O)_{1-x}$ ferrites sintered at 1100^0C/2hrs.

All the samples show crystallization with we defined diffraction patterns exhibited that all the samples were identified as a single phase of cubic spinel structure. The XRD patterns for all the samples were indexed for fcc spinel structure and the Bragg planes are shown in the patterns. The XRD patterns of the samples are given in Figure-1.The peaks (220), (311), (222), (400), (422), (551) and (440) correspond to spinel phase which are characteristic of spinel structures with a single phase. The lattice parameter 'a' corresponding to each plane was calculated by using the X-ray data. The average values of 'a' were found by plotting a against Nelson-Riley function.

The values of the lattice parameter obtained from each plane are plotted against Nelson-Riley function [22] $F(\theta)=\frac{1}{2}\left[\frac{Cos^2\theta}{Sin\theta}+\frac{Cos^2\theta}{\theta}\right]$, where θ is the Bragg's angle. A decrease in lattice constant is observed with the increasing of Fe-deficient content (x), in the lattice. This is indicates that the present system obeys the Vegard's law [23]. This may be due to Fe^{3+} ions having smaller ionic radius ($0.69A^0$) [24] than that of Ni^{+2}, Cu^{+2} and Zn^{+2} ions of ionic radius $0.78A^0$, $0.70A^0$ and $0.82A^0$ respectively [25], which when Zn^{+2} substituted resides on A-site and displaces all small ions from A site to B-site. This decrease

can be attributed to the vacancy created by Fe^{3+} deficiency with increasing its content. The unit cell is expected to reduce its size by contraction of the lattice resulting in decrease of lattice parameter gradually.

The calculated values of the bulk density and theoretical (or X-ray) density of the present ferrite system are listed in Table- 1. It is observed that bulk density is lower than the X-ray density. This may be due to the existence of pores which were formed and developed during the sample preparation or sintering process. The X-ray density slightly decreases with increasing Fe-deficiency and the bulk density increases continuously with increasing x-content.

The enhancement of bulk density is due to activated diffusion process triggered by the excess vacancies created by Fe^{3+} deficiency. It may be also be mentioned that reduction Fe^{2+} due to Fe^{3+} deficiency is expected to increase the resistivity of the samples. This density plays an important role on the magnetic properties especially on the structure sensitive property such as permeability and flux density. Table-1 shows the results of lattice parameter, theoretical density, and bulk density calculated porosity. It is observed from the Table-1 that porosity decreases monotonically with increasing Fe-deficiency in constant with bulk density which shows reverse behavior in figure-2

Table- 1 Data of the lattice parameter (a), X-ray density (d_x), bulk density (d_B), porosity (P%), molecular weight (M) of $(Ni_{0.28}Cu_{0.10}Zn_{0.62}O)\,(Fe_2O_3)_{1-x}$ samples sintered at 1100°C/2hrs

Fe-deficient content (x)	a (Å)	d_x (g/cm^3)	d_B (g/cm^3)	P%	M (g)
0.00	8.4382	5.21	4.52	13.24	239.02
0.02	8.4365	5.25	4.62	12	237.42
0.04	8.4338	5.22	4.80	8.04	235.82
0.06	8.4307	5.19	4.88	4.045	234.23
0.08	8.4275	5.16	4.93	4.04	232.63

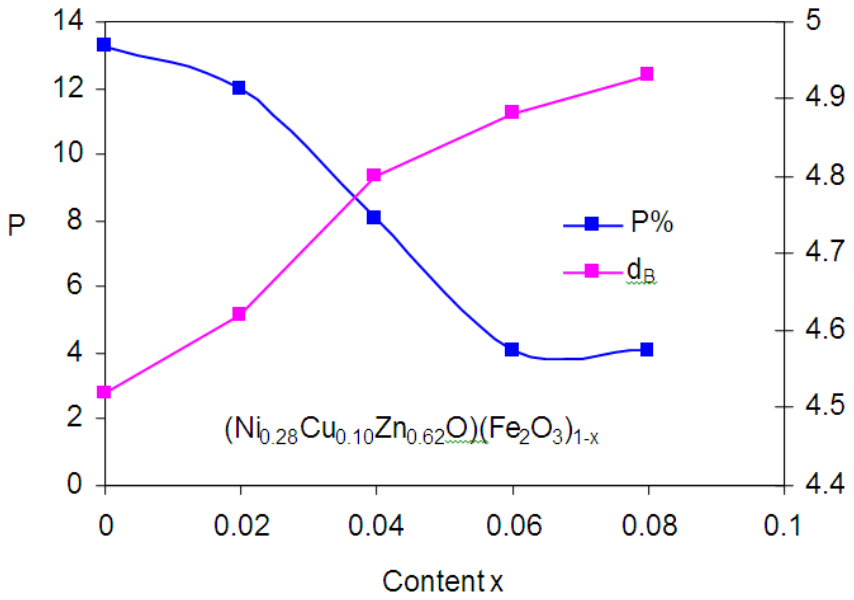

Figure-2 Bulk density and porosity as a function of Fe- deficient content (x)

The density of Fe, Ni, Cu and Zn are 7.87gm/c.c., 8.91gm/c.c. and 7.14gm/c.c. respectively. Zn acts as densification. It is known that Ni reduces densification rate of Ni-Cu-Zn ferrites; while Cu helps its densification [26]. This increase in densification is mainly due to decreasing of lattice parameter. Another reason might be due to the liquid phase formation in the ceramic

promoted material or atomic diffusion in the crystal [27]. The porosity which is intrinsic for any oxide material plays an important role in the deciding the magnetic and electrical properties.

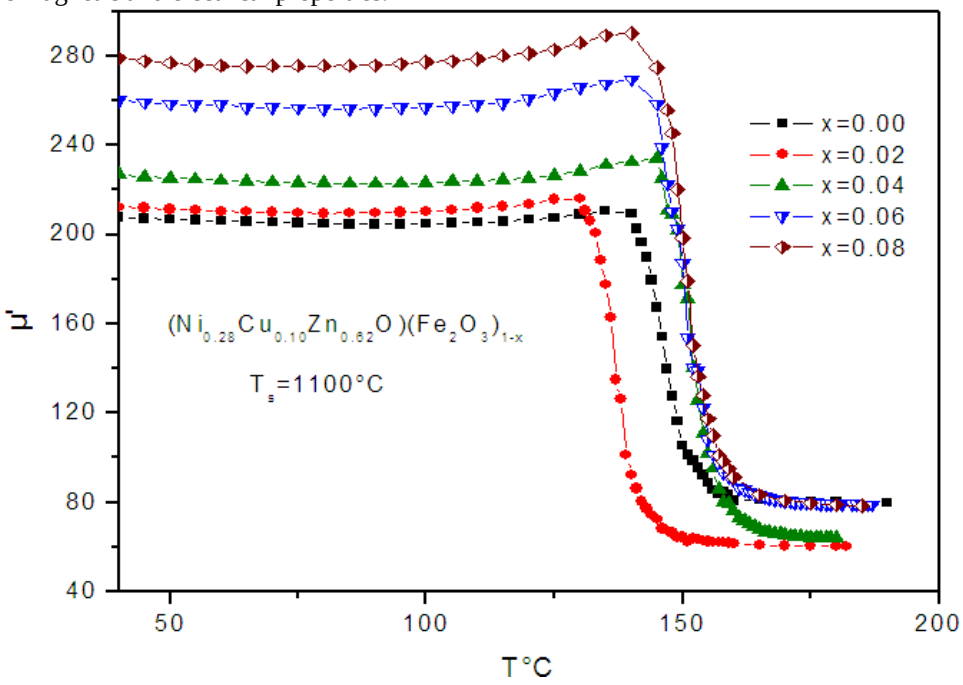

Figure-3 Variation of real part of permeability,μ′ with temperature of $(Ni_{0.28}Cu_{0.10}Zn_{0.62}O)(Fe_2O_3)_{1-x}$ ferrites sintered at 1100°C/2hrs.

Figure-3 shows the temperature dependence of initial permeability, μ', for the toroid shaped samples $(Ni_{0.28}Cu_{0.10}Zn_{0.62}O)(Fe_2O_3)_{1-x}$ ferrites where x = 0.00, 0.02, 0.04, 0.06 and 0.08 sintered at 1100°C/2hrs, which is measured at a constant frequency (100kHz) of an AC signal by using Impedance Analyzer. It is observed that the initial permeability increase with the increase in Fe-deficiency throughout the entire range of compositions, while it falls abruptly close to the Curie point.

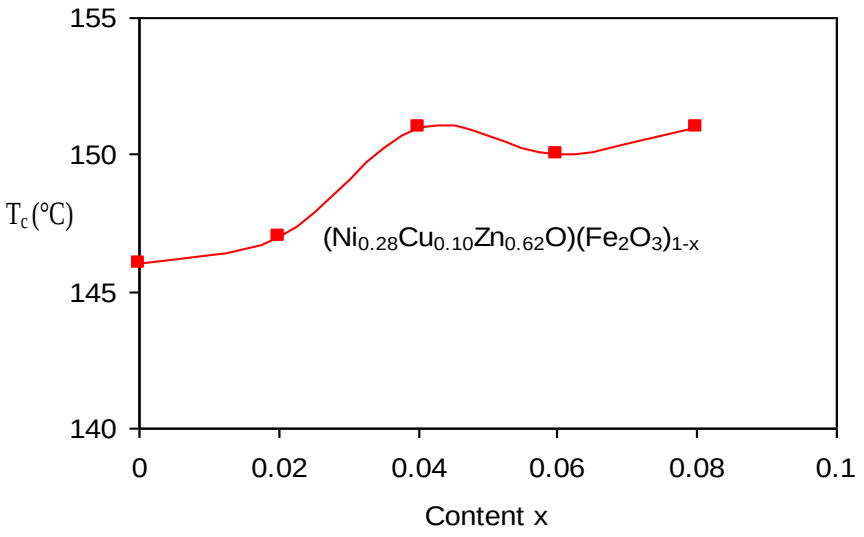

Figure-4: Variation of T_C with Fe-deficient (x) of $(Ni_{0.28}Cu_{0.10}Zn_{0.62}O)(Fe_2O_3)_{1-x}$ ferrites

This because Fe in these compositions not only increases the magnetic moments and but also lower anisotropy K_1 [28]. On the other hand, permeability increases with the decrease of K_1 as the temperature increases according to the relation

Table - 2 Data of Curie temperature (T_C) ($Ni_{0.28}Cu_{0.10}Zn_{0.62}O$) $(Fe_2O_3)_{1-x}$ ferrites

Fe- deficient Content X	T_s=1100°C
	T_c (°C)
0.00	146
0.02	147
0.04	151
0.06	150
0.08	151

$\mu' \propto \frac{M_S^2 D}{\sqrt{K_1}}$ [29 - 30]. It is observed from Figure-3 that the permeability falls sharply when the magnetic state of the ferrite samples changes from ferromagnetic to paramagnetic.

Figure-4 shows the variation of Curie temperature (T_C) with Fe-deficiency of ($Ni_{0.28}Cu_{0.10}Zn_{0.62}O$) $(Fe_2O_3)_{1-x}$ ferrites and the values are taken during the heating the sample. T_C is the transition temperature above which the ferrite material losses its magnetic properties. The T_C gives an idea of the amount of energy required to break up the long range ordering in the ferromagnetic material. The T_C mainly depends upon the strength of A – B exchange interaction. From the Figure-4 it is observed that T_C slowly and gradually increases with increasing of Fe – deficiency.

It is known that at T_C, the thermal energy wining over the exchange energy which results to disorder the system from an ordered one i.e. a ferromagnetic substance transforms to a paramagnetic one. T_C of ferrites is dependent on the strength of A –B exchange interaction [31]. As the Fe – deficiency is increased in the sample, the strength of the interaction of between the tetrahedral A –site and octahedral B-site might be increased which enhances the T_C.

The complex permeability is given by $\mu = \mu' - i\mu''$, μ' is the real permeability (in phase) and μ'' the imaginary permeability (90^0 out of phase). Complex permeability has been determined as a function of frequency, f up to 13MHz at room temperature for all the samples of series ($Ni_{0.28}Cu_{0.10}Zn_{0.62}O$) $(Fe_2O_3)_{1-x}$ ferrites by using the conventional technique based on the determination of the complex impedance of circuit loaded with toroid shaped sample. Figure-5 represents the results of the real part of the permeability μ' and Figure-6 imaginary part, μ'' as a function of frequency for the whole series of ferrite samples at 1100^0C for 2hrs.

From Figure-5 it is noticed that the real component of permeability, μ' is fairly constant with frequency up to certain frequency range and then falls rather rapidly to very low value at higher frequency. The permeability of composition with x = 0.00 to 0.08 were stable up to 2 – 3 MHz and the cut off frequencies of samples were evident from these figures that the initial permeability as a function of frequency increases with fe-deficiency (x-content), i.e. the permeability μ' increases monotonically with x – content. The constant value of permeability over a wide frequency range, which is named the zone of utility of ferrites, is desirable over various applications such a broad band transformer and wide band read-writes head for video recording [32]. From Figure -4 the range of operating frequency in the x = 0.04 and 0.06 samples are wider than that in the others which shows the compositional stability and quality of the ferrites samples.

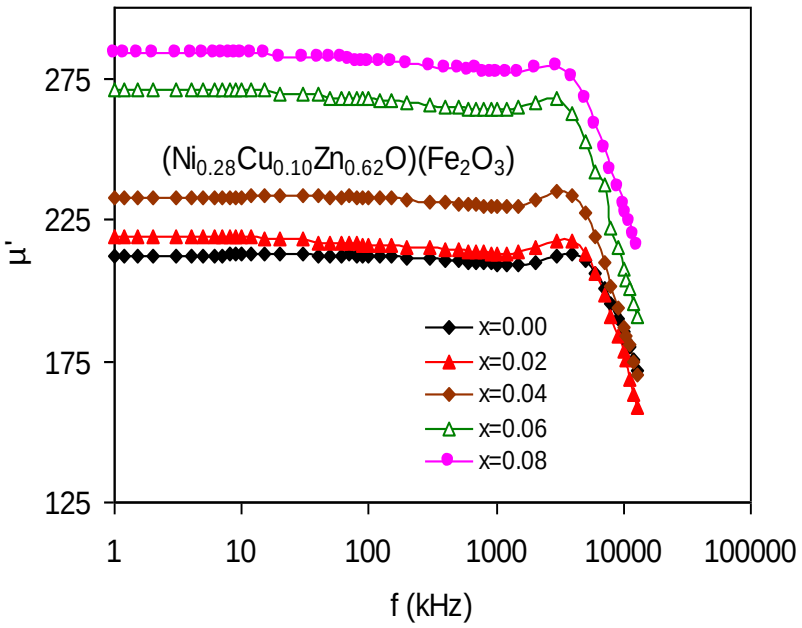

Figure-5 Variation of initial permeability with frequency of $(Ni_{0.28}Cu_{0.10}Zn_{0.62}O)(Fe_2O_3)_{1-x}$ ferrites sintered at 1100^0C/2hrs.

From the Figure-6, the imaginary permeability, $\mu^{//}$ first rises slowly and then increases quite abruptly making a peak at a certain frequency (called resonance frequency f_r), where the real component $\mu^{/}$ is failing sharply. This phenomenon is attributed to the ferromagnetic resonance. Resonance frequency (f_r) was determined from the maximum of imaginary permeability of the ferrites. It is observed from the Fig.-4.8 that the higher the permeability the lower the resonance frequency of the material. This really confirms with Snoek's limit [33]

$$f_r(\mu_i - 1) = \left(\frac{4}{3}\right)\gamma M_S \ ,$$

Where, f_r is the resonance frequency for domain wall motion, γ is the gyro magnetic ratio and M_S the saturation magnetization. This means that there is effective peaks are the results of the absorption of energy due to matching of the oscillation frequency of the magnetic dipoles and the applied frequency. Since the starting point of resonance frequency determine the upper limit of the operational frequency of any device, it predicts that the operational frequency range of the samples is greater than 6MHz. The resonance frequencies along with the permeability of the samples are listed in Table-3.

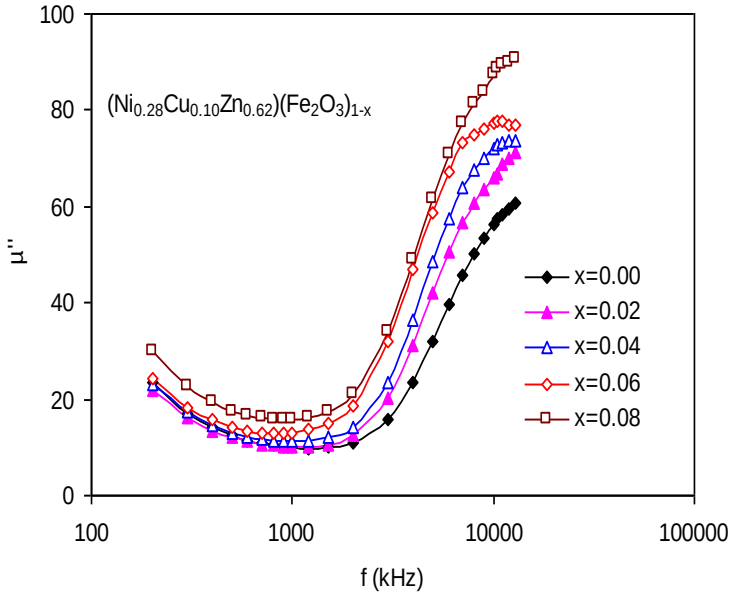

Figure-6 Complex imaginary permeability $\mu^{//}$ with frequency of $(Ni_{0.28}Cu_{0.10}Zn_{0.62}O)(Fe_2O_3)_{1-x}$ ferrites sintered at 1100^0C/2hrs.

Figure-6 shows that the variation of initial permeability at frequency 10kHz with Fe-deficient $(Ni_{0.28}Cu_{0.10}Zn_{0.62}O)(Fe_2O_3)_{1-x}$ ferrites sintered at 1100^0C for 2hrs. It was observed that the permeability increases slowly with increase in Fe-deficiency.

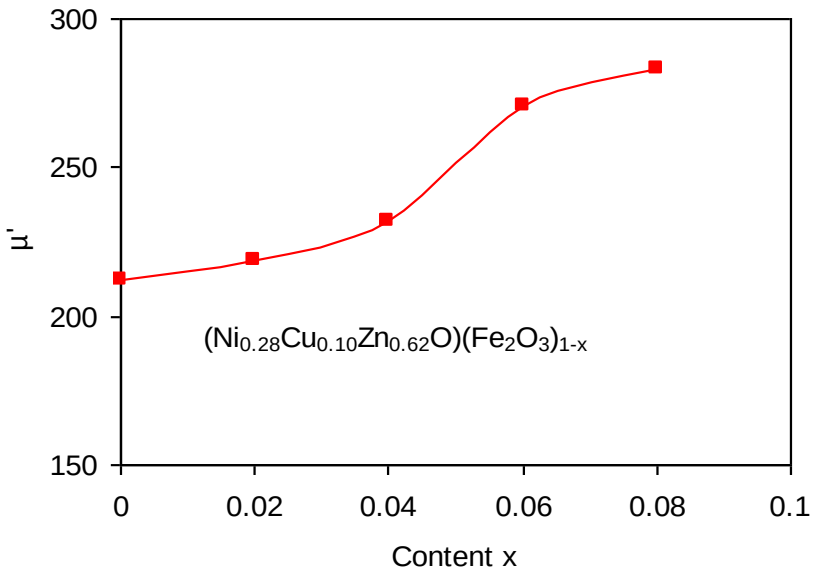

Figure-7 Variation of initial permeability, $\mu^{/}$ at frequency 10kHz with Fe-deficient of $(Ni_{0.28}Cu_{0.10}Zn_{0.62}O)(Fe_2O_3)_{1-x}$ ferrites sintered at 1100^0c/2hrs.

Table-3: Data for permeability ($\mu^{/}$), resonance frequency (f_r) and Snoek's limit ($\mu^{/}.f_r$) of $(Ni_{0.28}Cu_{0.10}Zn_{0.62}O)(Fe_2O_3)_{1-x}$ ferrites sintered at 1100^0C/2hrs.

Fe-deficient content (x)	Ts=1100°C		
	μ′ (10kHz)	f_r (MHz)	Snoek′s $\mu.f_r$(GHz)

0.00	212	13	2756
0.02	219	12	2628
0.04	272	12	2784
0.06	271	10.5	2846
0.08	283	10	2830

The increase of permeability with Fe-deficient is connected with increased magnetization, density, grain size and possible reduction of anisotropy energy. The initial permeability is closely corrected to the densification. An increase in the density of ferrites not only results in the reduction of magnetization field due to the presence of pores but also raise the spin rotational contribution, which in turn increases the permeability [34].

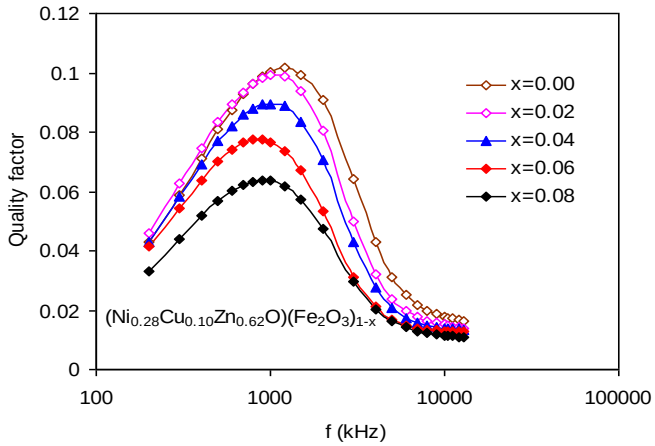

Figure-8 show the frequency dependence of relative quality factor (RQF) of the samples sintered at 1100^0C.

The variation of the relative quality factor with frequency showed a similar trend for all the samples. Q-factor increases with increases of frequency showing as peak and the decreases with further increase of frequency. It is seen that RQF deteriorates beyond 4.5MHz i.e., the loss tangent is minimum up to 4.5MHz and then it rises rapidly. The loss is due to lag of domain wall motion with respect to the applied alternating magnetic field and is attributed to various domain defects [35], which include non-uniform and non-repetitive domain wall motion, domain wall bowing, localized variation of flux density, nucleation and annihilation of domain walls. This phenomenon is associated with the ferromagnetic resonance within the domains [36] and at the resonance maximum energy is transferred from the applied magnetic field to the lattice resulting in the rapid decreases in RQF. The peak corresponding to maxima in Q-factor shifts to lower frequency range as Fe-deficiency increases, sample with x = 0.00 possess the maximum value of quality factor.
Figure-8 Variation of RQF as a function of frequency of $(Ni_{0.28}Cu_{0.10}Zn_{0.62}O)(Fe_2O_3)_{1-x}$ ferrites sintered at 1100^0C/2hrs.

Both ferro- and ferromagnetic materials differ widely in the case with which they can be magnetized. If a small applied field suffices to produce saturation the material is said to be magnetically soft. Saturation of some other material, which will in general have a different value of M_S, may require very large fields. Such a material is magnetically hard. Sometimes the same material may be either magnetically soft or hard, depending on its physical condition: thus curve (a) might relate to a well annealed material, and curve (b) to the heavily cold worked state.

Thus derivative $\left(\frac{dB}{dH}\right)$ is unity beyond the point B_S, called the saturation induction. However, the slope of these lines does not normally appear to be unity, because the B and H scales are usually quite different.

Figure-9 represents the B - H loops at room temperature were measured with B - H loop tracer at constant frequency (f = 1kHz) and applied field H = 0 – 15Oe for the whole series of $(Ni_{0.28}Cu_{0.10}Zn_{0.62}O)(Fe_2O_3)_{1-x}$ ferrites where x = 0.00, 0.02, 0.04, 0.06 and 0.08 sintered at 1100^0C/2hrs. From these loops the remanence induction (B_r), saturation induction (B_S) and the coercive force (H_C) were determined. These results are shown in Table-4.

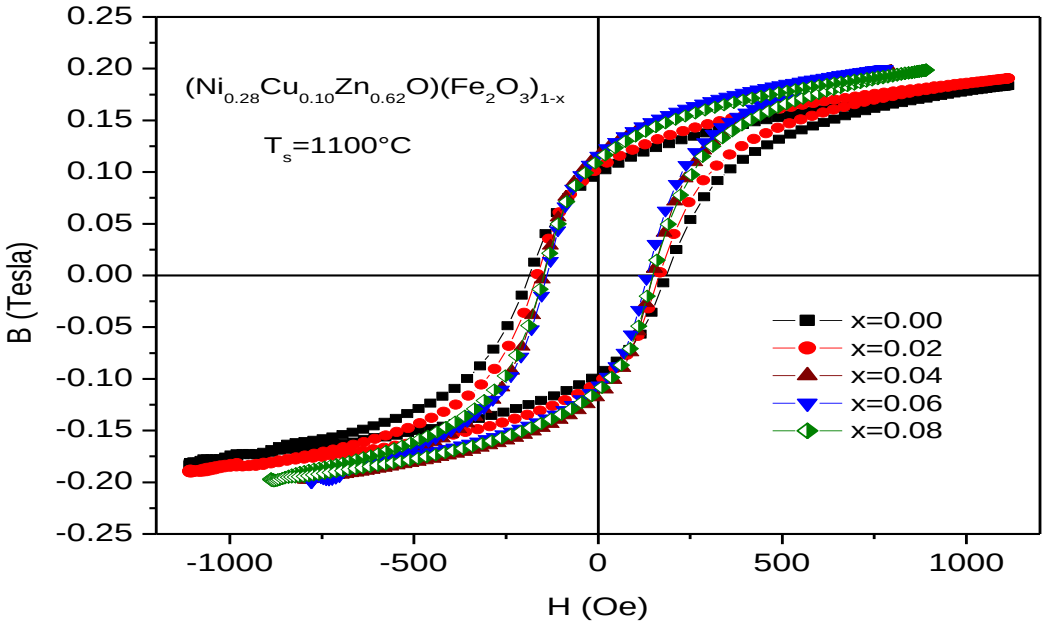

Figure-9 Magnetic hysteresis graphs of $(Ni_{0.28}Cu_{0.10}Zn_{0.62}O)(Fe_2O_3)_{1-x}$ ferrites with x sintered at 1100^0C/2hrs.

It is observed that the B_r and B_S both increase with x-content. For high permeability material a low coercivity is a prime requirement which is fulfilled in the present study. Since permeability is inversely related to coercivity i.e., $\mu' \propto \frac{1}{H_c}$. Again a high B_S is also a requirement for high permeability which is also manifested in the studied sample. Figure-10 shows the dependence of permeability μ' and coercivity, H_c with x content. And excellent correlation between μ' and H_c is observed.

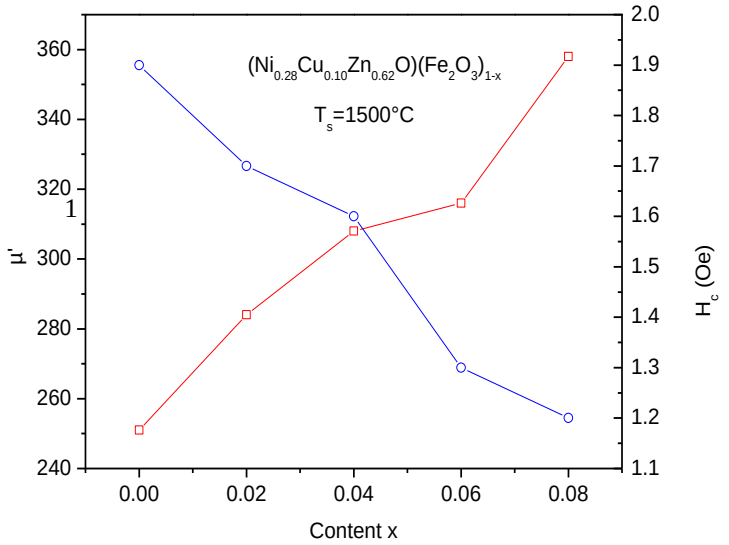

Figure-10 Magnetic hysteresis graph of $(Ni_{0.28}Cu_{0.10}Zn_{0.62}O)(Fe_2O_3)_{1-x}$ ferrites with x sintered at 1100^0C/2hrs at constant frequency f = 1kHz and μ' and H_c versus x-content.

The low coercive force and higher permeability confirms that the development of soft magnetic characteristic properties of Ni-Cu-Zn ferrite with increasing Fe-deficiency, which is well known as soft magnetic materials from application point of view. The increase of Fe-deficiency decreased the coercive field and the hysteresis losses, increase the samples magnetization and permeability. B_s is found to increase with increasing Fe-deficient. The different values of retantivity and $\frac{B_r}{B_s}$ ratio observed are interpreted in a quantitative way by means of domain theory. The predominant losses in Ni-Cu-Zn ferrite are hysteresis and eddy current at operating frequencies lower than the relaxation frequency of the wall displacement. The values of maximum flux density, coercive field, and hysteresis loss of the system has been found with x = 0.08.

Table-4 The experimental values of coercive force (H_c), remanence induction (B_r), saturation induction (B_s), $\left(\frac{B_r}{B_s}\right)$ ratio and losses of $(Ni_{0.28}Cu_{0.10}Zn_{0.62}O)(Fe_2O_3)_{1-x}$ samples at room temperature with constant frequency (f = 1kHz) at sintering temperature 1100^0C/2hrs.

Fe-deficient content (x)	H_C (Oe)	B_r (kG)	B_s (kG)	B_r/B_s	Losses (W/kg)
0.00	2.34	0.97	1.84	0.53	22.13
0.02	2.08	1.03	1.90	0.54	21.11
0.04	1.87	1.17	1.97	0.59	20.39
0.06	1.87	1.21	2.13	0.56	23.64
0.08	1.94	1.10	2.10	0.52	23.85

If H is reduced to zero after saturation has been reached in the positive direction, the induction in a ring specimen will decrease from B_s to B_r, called the retentivity or residual induction. If the applied field is then reversed, reversing the current in the magnetizing winding, the induction will decrease to zero when the negative applied field equals the coercivity, H_c. The B - H loop of this sample is wide and almost reversible.

The room temperature magnetic hysteresis loop of the samples has been measured and is presented in Figure-9 The hysteresis loops do not show any noticeable hysteresis effect. All samples exhibited low coercivity values inducting that all the samples being to the family of soft ferrites. Figure-10 shows the variation of magnetization of the $(Ni_{0.28}Cu_{0.10}Zn_{0.62}O)(Fe_2O_3)_{1-x}$ ferrites as a function of applied magnetic field for various samples where x = 0.00, 0.02, 0.04, 0.06 and 0.08. It is observed from the Figure-11 that virgin saturation magnetization M_s increases up to x = 0.06 and then decrease slightly with x content

The insignificant decrease of M_s may be experimental uncertainty. The observed variation in M_s can be explained on the basis of cation distribution and the exchange interactions between A and B sites. The initial increase in M_s with increased Fe-deficient is due to the increase of resultant sub lattice magnetic moment which can be explained on the basis of Neel's two sub lattice model. Neel [37] considered three types of exchange interactions between unpaired electron of two ions lying in A and B sites. In perfect ferrites, the A - A, B - B and A - B nearest neighbor exchange coupling are normally anti ferromagnetic and the A - B exchange coupling is usually heavily predominant.

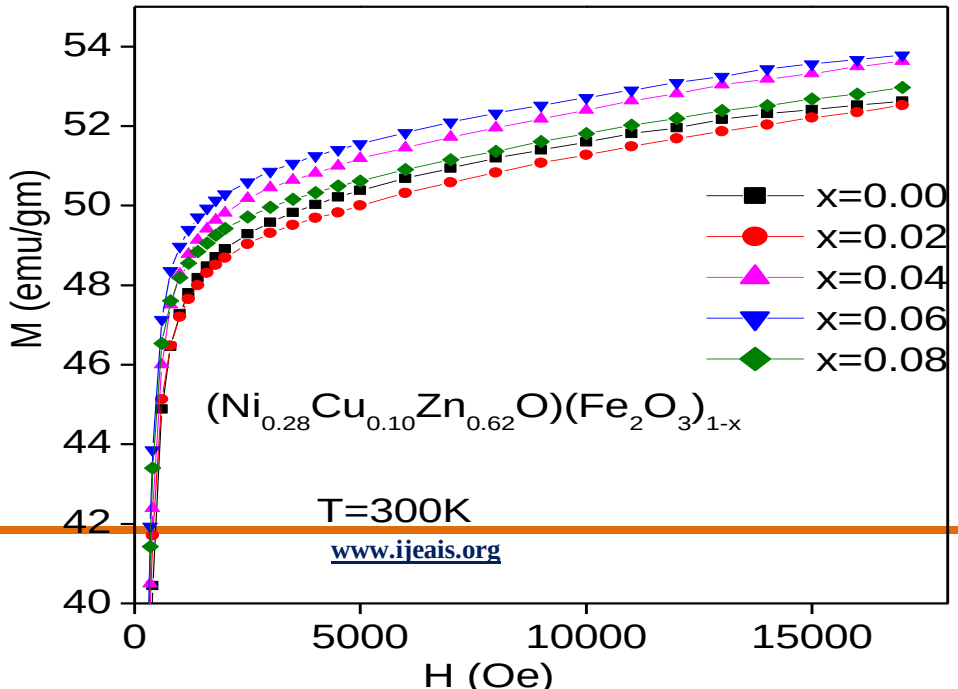

Figure-10 Field dependence of magnetization at virgin state of $(Ni_{0.28}Cu_{0.10}Zn_{0.62}O)(Fe_2O_3)_{1-x}$ ferrites where x = 0.00, 0.02, 0.04, 0.06 and 0.08 sintered at 1100^0C/2hrs at constant frequency f = 1kHz.

The net magnetization is therefore the difference between the magnetic moments of B and A sub lattices, i.e. $M = M_B - M_A$ and will normally be parallel to the B-sub lattice magnetization because the number of cations on B-sites is twice the number of cations on A-sites. The magnetization of each composition depends on the distribution of Fe^{3+} ions between the two sub lattices A and B, where the Ni^{2+} and Zn^{2+} ions are non magnetic. It is mentioned that $CuFe_2O_4$ and $NiFe_2O_4$ ferrite are known as inverse ferrite, where Cu^{2+} and Ni^{2+} ions are located on B-sites.

The substitution will lead to increase Fe^{3+} ions on the B-sites and consequently the magnetization of the B-sites will increase. At the same time the magnetization of A-site will decrease according to the decrease of the Fe^{3+} ions on A-site. So the net magnetization will increase accordingly up to x = 0.06 as shown in Figure-11.

Figure-11 shows the temperature dependence of saturation magnetization measured with an applied magnetic field of H = 5kOe. It is observed that magnetization, M_s decreases monotonically with increasing temperature and finally tends toward zero above the Curie temperature, T_c . The show decreases of magnetization unlike ferromagnet where much sharper fall of M_s is observed that at $T = T_c$. From the Figure-11, it is observed that at low temperature magnetization increases slightly with increasing x-content.

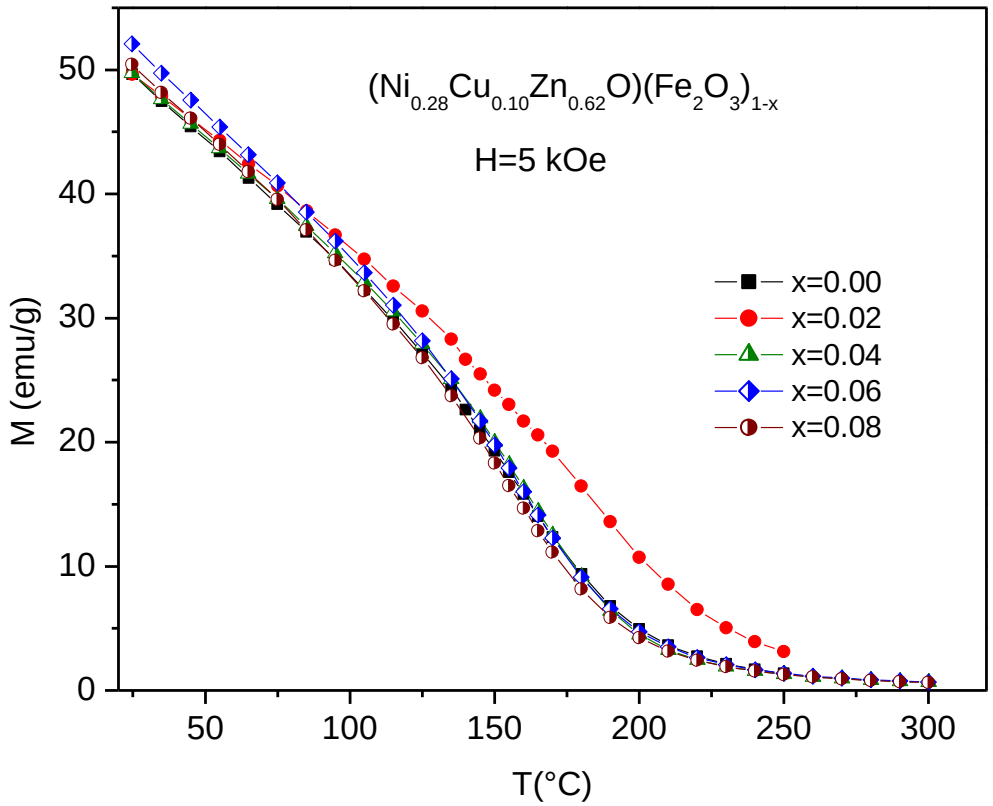

Figure-11 Temperature dependences of magnetization of $(Ni_{0.28}Cu_{0.10}Zn_{0.62}O)(Fe_2O_3)_{1-x}$ ferrites with an applied field 5kOe

Electrical DC resistivity is an important electrical property of ferrites in high frequency application. Figure-12 shows the room temperature values of resistivity versus Fe-deficient of samples of series $(Ni_{0.28}Cu_{0.10}Zn_{0.62}O)(Fe_2O_3)_{1-x}$ ferrites by using a keithely Electrometer. For measurements, the pellet shaped samples were coated with silver paint on the both surfaces of each sample to obtain good ohmic contact. The DC resistivity is found to increase vary fast up to x = 0.02 with Fe-deficient. Resistivity is found to increase slowly with further addition of Fe-deficient. Resistivity is found to decrease with further increase of Fe-deficient. This decrease of resistivity may be attributed to the entrapped of intragranular porosity. Sankpul et. al. and Shaikh et. al. measured resistivity as a function of composition in their work on Ni-Cu and Li-Cu ferrites [38– 39].

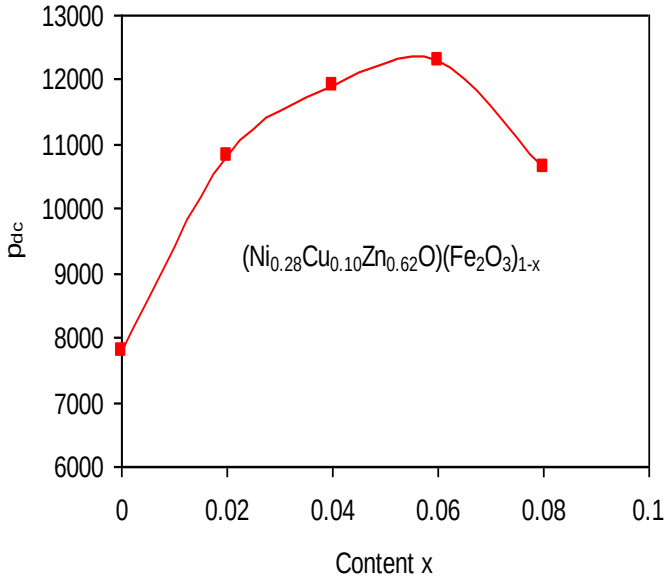

Figure-12 Room temperature DC resistivity as a function of Fe-deficient content (x) of $(Ni_{0.28}Cu_{0.10}Zn_{0.62}O)(Fe_2O_3)_{1-x}$ ferrites sintered at 1100^0C/2hrs.

The highest value of DC resistivity for x = 0.06 same is observed 12.3×10^3 Ω-cm and values are shown in Table-5. The observed decrease in resistivity with the increase of Fe-deficient has been related to the decrease of porosity since pores are non-conductive. This trend could be attributed to the high activation energy, which is associated with high resistivity at room temperature.
This very large resistivity means in turn that an applied alternating magnetic field will not induce eddy currents in a ferrite. This property makes ferrite the best magnetic materials for high frequency applications where power losses from eddy currents must be minimized. Figure-13 shows the frequency dependence of AC resistivity and values are shown in table-5. A large decrease in resistivity was found with increasing Fe-deficient. All the samples show the significant dispersion with frequency which is the normal ferromagnetic behavior. The AC resistivity of the composition also decreased due to enhancement of Fe^{2+} ion concentration. It means that the decrease in AC resistivity with Fe-deficient was due to the increase of electrons in the ferrites.

Table-5: AC and DC resistivity at 100 kHz of $(Ni_{0.28}Cu_{0.10}Zn_{0.62}O)(Fe_2O_3)_{1-x}$ ferrites sintered at 1100^0C/2hrs.

X	DC Resistivity ρ_{dc} Ω-cm	AC Resistivity	
		ρ_{ac}, Ω-cm 1kHz	ρ_{ac} Ω-cm 100kHz
0	7.8×10^3	3.1×10^4	1.4×10^3
0.02	10.8×10^3	6.3×10^4	2.3×10^3
0.04	11.9×10^3	7.7×10^4	3.7×10^3
0.06	12.3×10^3	9.1×10^4	5.6×10^3
0.08	10.6×10^3	3.7×10^4	4.1×10^3

The resistivity of all the composition decreased with the increasing frequency. The resistivity (ρ_{ac}) was calculated as per equation(1)

$$\rho_{ac} = \frac{1}{\omega \varepsilon_0 k' \tan \delta}$$

$$\rho_{ac} = \frac{A}{2\pi f \tan \delta C t} \qquad (1)$$

The resistivity was primarily dependent on the frequency and was found to be inversely proportional that was why resistivity decreases with the increase in frequency. The low frequency region corresponds to high resistivity due to grain boundaries whereas high frequency ranges corresponds to low resistivity due to the grains [40].

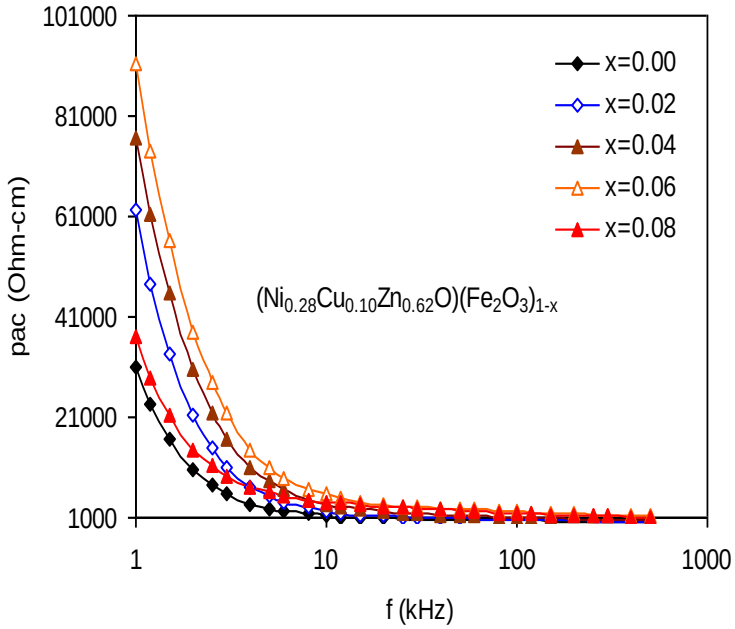

Figure-13 AC resistivity as a function of frequency of $(Ni_{0.28}Cu_{0.10}Zn_{0.62}O)(Fe_2O_3)_{1-x}$ ferrites sintered at 1100^0C/2hrs.

Figure-14 shows the variation of dielectric constant, $\varepsilon^{/}$ with frequency for different composition of $(Ni_{0.28}Cu_{0.10}Zn_{0.62}O)(Fe_2O_3)_{1-x}$ ferrites sintered at 1100^0C/2hrs for 1kHz to 13MHz at room temperature. It can be seen from the figure that the dielectric constant is found to decrease continuously with increasing frequency for all the specimens exhibiting a normal dielectric behavior of ferrites. The dielectric dispersion is rapid at lower frequency region and it remains almost independent at high frequency side. The incorporation of Fe into these ferrites has no pronounced effect on the dielectric constant in high frequency, but significantly decreases the dielectric constant in the low frequency range.

The type of behavior was observed in a number of ferrites such as Li- Co ferrites [41], Cu – Cd ferrites [42], Ni–Cu–Zn ferrites [43], Mg–Cu–Zn ferrites [44- 45]. The dielectric behavior of ferrites may be explained on the basis of the mechanism of the dielectric polarization process and is similar to that of the conduction process. The electronic $Fe^{2+} \leftrightarrow Fe^{3+}$ gives the local displacement of electrons in the direction of applied electric field, which induces the polarization in ferrites [45].The magnitude of exchange depends on the concentration Fe^{2+}/Fe^{3+} in pairs present on B-site for the present ferrite. All the samples have high value of $\varepsilon^{/}$ in the order of 10^5 at low frequencies. This could be explained using koop's phenomenological theory [46] which was based on the Maxwell-Wagner model [47 – 48] for the inhomogeneous double layer dielectric structure. The first layer is the fairly well conducting large ferrite grain which is separated by the second thin layer of the poorly conducting grain boundaries. The grain boundaries of the lower conductivity were found to be ferrite at lower frequencies while ferrite grains of high conductivity are effective at high frequency.

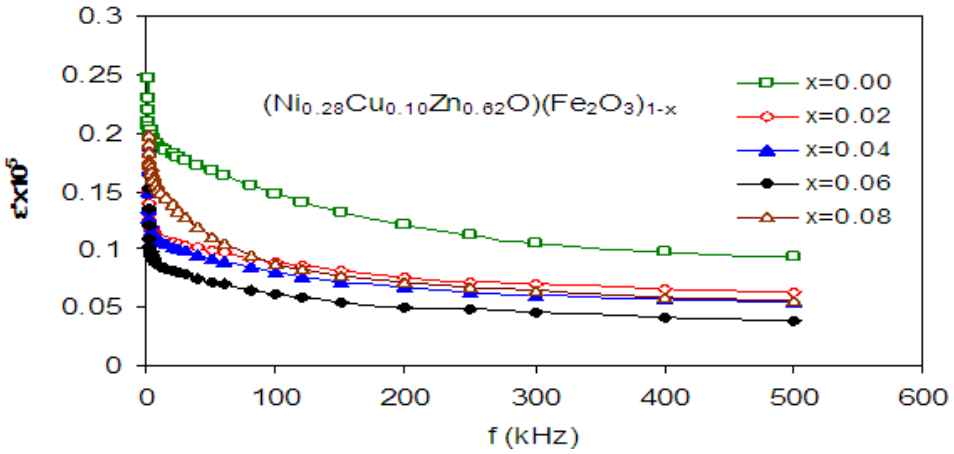

Figure-14 Dielectric constant as a function of frequency of the ferrite system of $(Ni_{0.28}Cu_{0.10}Zn_{0.62}O)(Fe_2O_3)_{1-x}$ ferrites sintered at 1100^0C/2hrs.

4. Conclusion

The present work is focused on the synthesis, characterization and detail study of structure, electrical and transport magnetic properties of Fe-deficient of $(Ni_{0.28}Cu_{0.10}Zn_{0.62}O)(Fe_2O)_{1-x}$ ferrites where x = 0.00, 0.02, 0.04, 0.06 and 0.08 samples using standard double sintering ceramic method, sintered at 1100^0C for two hours. The X-ray diffraction confirmed the single phase cubic spinel structure of the samples. The lattice constant decreases with increasing Fe-deficient content obeying Vegard's law. Bulk density is found to increase while porosity decreases with decreasing Fe-deficient content.

Curie temperature slightly increases linearly with the addition of Fe-deficient content possibly due to weakening of A – B exchange interaction. This happened due to increase linkage between the magnetic ions and exchange coupling that determines the magnitude of the Curie temperature. The initial permeability gradually increases with increasing x-content at constant sintering temperature 1100^0C/2hrs. The initial permeability is constant up to 2 – 4.5MHz region dependent on sintering temperature. Grain size has a great influence on the domain wall contribution and hence on permeability is constant up to 2 - 3 MHz region dependent on sintering temperature. Ferromagnetic resonance f_r shifts to lower frequency with increasing of permeability validating Snoek's relation $\mu_i.f_r$ = constant.

Saturation magnetizations are found to increase with increasing Fe-deficient. This may be due to modified cation distribution on two sub lattice. The low field hysteresis parameter such as coercivity (H_c) decreases with increasing Fe-deficiency. The remanance (B_r) and flux density (B_s) increases gradually with Fe-deficient. Increase of H_c comes from the enhancement of pinning force between domain walls and grain boundaries resulting from smaller grain size. The DC electrical resistivity increases with increasing Fe-deficient content up to x = 0.06 and thereafter decreases. The AC electrical resistivity decrease with increase in frequency. Dielectric constant decreases with increasing frequency exhibiting normally dielectric behavior of ferrites. Based on the experimental results in terms of soft magnetic properties it may be concluded that optimum composition of Fe-deficient $(Ni_{0.28}Cu_{0.10}Zn_{0.62}O)(Fe_2O)_{1-x}$ ferrites series x = 0.06 sintered at 1100^0C/2hrs with high initial permeability of 271, low H_c of 1.87Oe and minimum hysteresis loss of 23.64W/kg.

Finally Soft ferrite materials are extensively used in inductor cores which form a basic requirement in modern technology. Ni – Cu - Zn ferrites are suitable for these devices for future. Fabrication and characterizations of multilayer chip inductor using improved Ni - Cu –Zn ferrites is of high demand.

Acknowledgment

One of the authors (M. A. Hossain) is thankful to Khulna University of Engineering & Technology (KUET), Khulna, Bangladesh for the financial support. The authors are also grateful to the Materials Science Division of Atomic Energy Centre, Dhaka (AECD), Bangladesh for allowing their facilities to prepare the samples and to utilize the laboratory facilities for various measurements. Financial support from International Program in Physical Science (IPPS), Uppsala University, Sweden for this work is highly acknowledged.

REFERENCES

[1] S. Hilpert; Ber. Deutseh Chem. Gas. Bd2, 42, 2248, 1909.

[2] A Verma, T. C. Goel, R. G. Mendiralta, R. G. Gupta; 1999, "High-resistivity Nickel-Zinc ferrites by the Citrate precursor method"; J. Magn. Magn. Mater. Vol.192, pp.271-276.

[3] T. Nakamura, T. Miyaonoto, Y. Yamada; 2003, "Complex Permeability Spectra of Polycrystalline Li-Zn ferrite and application of EM-Wave absorber"; J. Magn. Magn. Mater. Vol.256, pp.340-347.

[4] A. Lakshman, K. H. Rao, R. G. Mendiratta; 2002, "Magnetic Properties of In3+ and Cr3+ substituted by Mg-Mn ferrites"; J. Magn. Magn. Mater. 235 (2001) 159.

[5] J. L. Snoek; "New Development Ferromagnetic materials'; Elsevier Publ. Co. N. Y. (1947).

[6] L. Neel; "Properties Magnetique des ferrites: Ferimagnetism et Antiferromagnetism"; Annels de Physique, 3(1948) 137.

[7] T. Nakamura; "Low Temperature Sintering of Ni – Cu- Zn ferrite and its Permeability Spectra"; J. Magn. Magn. Mater. 168 (1997) 285 – 291.

[8] T. Nakamura, T. Tsutaka, K. Hatake Yana; "Frequency dispersion of permeability in ferrite c omposite materials"; J. Magn. Magn. Mater, 138 (1994) 319.

[9] E. Rezlescu, N. Reszlescu, P. D. Popa, C. Pasnicu, M. L. Craus; Mat. Res. Bull. 33(6) (1998) 915.

[10] K. O. Low, F. R. Sale; "Sintering of gel-derived Ni – Cu- Zn ferrites"; Ferrites Proceedings of ICF 8, Kyoto, Tokyo, Japan; The Japan Society of Power and Powder Metalurgy, 2000, pp. 548 – 550.

[11] Kin O. Low, Frank R. Sale; "Electromagnetic properties of gel-dervied Ni- Cu- Zn ferrites"; J. Magn. Magn. Mater. 246 (2002) 30-35.

[12] G. Goev, V. Masheva, L. Ilkov, D. Nihtianova, M. Mikhov; Proceedings of the 5th General Conference of the Balken Physical Union BPU – 5 (2003) 687.

[13] K. O. Low, F. R. Sale; J. Magn. Magn. Mater. 256 (2003) 221.

[14] L. B. Kong, Z. W. Li, G. Q. Lin and Y. B. Gan; "Magneto-dielectric properties of Mg-Cu-Co ferrite ceramics: II Electric, dielectric and magnetic properties", J. An. Ceram. SOC 90(7) (2007) 2104.

[15] S. K. Sharma, Ravi Kumar, Shalendra Kumar, M. Knobel, C. T. Meneses, V. V. Siva Kumar, V. R. Reddy, M. Shingh and C. G. Lee; "Role of inter particle interactions on the magnetic behavior of Mg0.95Mn0.05Fe2O4 ferrite nano particle"; J. Phys. Condens. Matter 20(2008) 235-214.

[16] Soilah Zahi, Mansor Hashim and A. R. Daud; "Synthesis, Magnetic and microstructure of Ni-Zn ferrite by Sol-gel technique"; J. Magn. Magn. Mater. 308(2007) 177.

[17] M. A. Hakim, D. K. Saha and A. K. M. Fazle Kibria; "Synthesis and temperature dependent structural study of nanocrystalline Mg-ferrite materials"; Bang. J. Phys. 3(2007) 57.

[18] A. Bhaskar, B. Rajini Kanth and S. R. Murthy; "Electrical properties of Mn added Mg-Cu-Zn ferrites prepared by microwave sintering method"; J. Magn. Magn. Mater. 283(2004) 109.

[19] ZhenXing Yue, Ji Zhou, Longtu Li and Zhilun Gui; "Effects of MnO2 on the electromagnetic properties of Ni-Cu-Zn ferrites prepared by Sol gel auto-combustion"; J. Magn. Magn. Mater. 233(2001) 224.

[20] C. W. Chen, Magnetism and Metallurgy, Soft Mag. Mat., North-Holland Pub. Com. XV, 288(1977).

[21] A Goldman, Handbook of Modern Ferromagnetic Materials, Kulwer Acad. Pub, Boston, U.S.A. 1999.

[22] J. B. Nelson, D. P. Riley; "An experimental investigation of extrapolation methods in the derivation of accurate unit-cell dimension of crystals"; Proc. Phys. SOC London 57 (1945) 160.

[23] L. Vagards; "Die constitution der mischkristalle und die raumfullung der atome"; Z. Phys. 5 (1921) 17.

[24] J. Smit, H. P. J. Wijn; Ferrites Wiley New York, (1959) p.143.4.4

[25] L. John Berchamans, R. Kalali Selvan, P. N. Selva Kumar and C. O. Augustin; "structural and electrical properties of Ni1-xMgxFe2O4 synrhesized by citrate gel process', j. Magn. Magn. Mater. 279 (2004) 10.

[26] K. O. Low, F. R. Sale; J. Magn. Magn. Mater. 256 (2003) 221.

[27] C. R. Foschini, L. Perazolli, J. A. Varela; J. Mat. Sci. 39(20040 5825.

[28] A. Goldman; "Hand book of Modern Ferromagnetic Materials" Kulwer Academic Publishers, Boston, USA, 1999.

[29] G. C. Jains, B. K. Das, R. S. Khandyja and S. C. Gupta; "Effect of itergranular porosity of initial permeability and coercive force in a manganese zinc ferrite"; J. Mater. Sci. II (1976) 1335.

[30] S. Chikazumi; "Physics of Magnetism"; John Wiley and son, Inc. New York 1966.

[31] B. Jeyadevan, C. N. Chinnasamy, K. Shinoda, K. Tohji; "Mn-Zn ferrite with higher magnetization for temperature sensitive magnetic fluid"; J. Appl. Phys., Vol.93 (2003) pp.8450.

[32] A. Verma, R. Chatterjee; "Effect of zinc concentration on the structural, electrical and magnetic properties of mixed Mn-Zn and Ni-Zn ferrites synthesized by the citrate precursor technique"; J. Magn. Magn. Mater. 306(2006) 313-320.

[33] J. L. Snoek; "Dispersion and absorption in magnetic ferrites at frequencies above on MC/S"; Physica, 14(4) (1948) 207.

[34] J. J. Shrotri, S. D. Kulkarni, C. E. Deshpande, S. K. Date; "Effect of Cu substitution on the magnetic and electrical properties of Ni-Zn ferrite synthesized by soft chemical method"; Mater. Chem. Phys. 59 (1999) 1.

[35] K. Overshott; "The causes of the anomalous cross in amorphous ribbon materials"; IEEE Trans. Magn. 17 (1981) 2698.

[36] F. G. Brockman, P. H. Dowling and W. G. Steneck; "Dimensional effects resulting from a high dielectric constant found in a ferromagnetic ferrite"; Phys. Rev. 77 (1950) 85.

[37] I. Neel; Ann. Phys. 3(1948) 137.

[38] E. A. Schwabe and D. A. Campell; J. Appl. Phys. 34, 1251 (1963).

[39] Igarashi H. and Dkazaki; K. J. Am. Cer. SOC 60[1-2], 51, (1977).

[40] Ž. Cvejić, S. Rakić, S. Jankov, S. Shuban, A. Kapor; Processing and Application of Ceramics; 2(1) (2008) 53.

[41] Nutan Gupta, S. C. Kashyap and D. C. Dube; "Dielectric and Magnetic properties of Citrate route processed Li-Co Spinel ferrites"; Phys. Stat. Solidi(a) 204(7) (2007).

[42] C. B. Kolekar, P. N. Kamble, S. G. Kulkarni and A. S. Vaingankar; "Effect of Gd3+ substitution on dielectric behavior and copper-cadmium ferrites"; J. Matter. Sci. 30(1995) 5784.

[43] Zhenxing Yue, Zhou Ji, Zhilun Gui and Longtu Li; "Magnetic and electrical properties of low temperature sintered Mn-doped Ni-Cu-Zn ferrites"; J. Magn. Magn. Mater. 264(2003) 258.

[44] S. S. Bellad and B. K. Chougula; "Composition and frequency dependent dielectric properties of Li-Mg-Ti ferrites"; Mater. S. Chem. Phys. 66(2000) 58.

[45] A Bhaskar, B. Rajini Kanth, S. R. Murthy; "Electrical properties of Mn added Mg-Cu-Zn ferrites prepared by microwave sintering method"; J. Magn. Magn. Mater. 283(2004) 109.

[46] Zhenxing Yue, Zhou Ji, Longtu Li, Xiaolui Wang and Zhilun Gui; "Effect of copper on the electromagnetic properties of Mg-Zn-Cu ferrites prepared by Sol-gel auto-combustion method"; Mater. Sci. Eng.B 86(2001) 64.

[47] Maxwell J.; 1873, Electricity and Magnetism; Vol.1 Oxford University Press. London Wanger K 1913 Ann. Phys. 40 817.

[48] p. venugopal Reddy, T. Seshagiri Rao; "Dielectric behavior of mixed Li-Ni ferrites at low frequencies"; J. Less. Common Met. 86 (1982) 255.

[49] B. Kumar Kunar, G. Srivastava; "Dispersion observed in electrical properties of titanium substituted lithium ferrites"; J. Appl. Phys. 75 (1994) 6115.